Mechanics of Advanced Composite Structures Vol (Year), Serial Number, First page – Last page

Semnan University

Mechanics of Advanced Composite Structures

Journal homepage: https://macs.semnan.ac.ir/

ISSN: 2423-7043

Research Article

Parametric Effects and Regression-Based Optimization of Drilling Performance in Glass Fiber-Reinforced Polymer Composites

Farzad Ahmadi Khatir [a]*, Vahid Majidi [a], Vahid Abedini [a], Masoud Mahmoodi [a]

[a] *Faculty of Mechanical Engineering, Semnan University, Semnan, Iran*

ARTICLE INFO

Article history:

Received: 2026- -
Revised: 2026- -
Accepted: 2026- -

Keywords:

GFRP composites;
Drilling;
Push-out Delamination;
Thrust force;
Torque;
Process optimization;
Design of experiments;

ABSTRACT

Glass fiber-reinforced polymer (GFRP) composites have gained widespread application in aerospace, automotive, and marine industries due to their superior mechanical properties. However, drilling-induced delamination remains a critical challenge that compromises structural integrity and assembly reliability. Among the two primary delamination modes (peel-up at the entry and push-out at the exit), push-out delamination is typically more severe and governs the structural performance of drilled components; therefore, this study focuses on exit-side delamination. This study investigates the influence of drilling parameters—spindle speed (500–1000 rpm), feed rate (0.05–0.2 mm/rev), and drill point angle (90°–130°)—on thrust force, torque, and delamination factor during GFRP machining. Experimental tests were conducted using HSS-Co 5% drills on 2.2 mm thick laminates fabricated via room-temperature consolidation, with force and torque data acquired using a Kistler 9255B dynamometer. Delamination was quantitatively assessed through digital image processing based on the ratio of damaged area to nominal hole area. Analysis of variance (ANOVA) confirmed the statistical significance of the developed regression models (Adjusted $R^2 > 0.90$). Results revealed that feed rate exerts the most dominant influence on all response variables, while spindle speed demonstrates a nonlinear effect on force and torque but consistently reduces delamination at higher values. Increasing drill point angle effectively minimizes torque but exhibits marginal influence on thrust force and delamination. Multi-response optimization yielded an optimal drilling condition of 110° point angle, 720 rpm spindle speed, and 0.05 mm/rev feed rate, balancing minimal machining forces with suppressed delamination. The findings provide practical guidelines for enhancing hole quality in GFRP components and contribute to the development of damage-free drilling strategies for advanced composite structures.

* **Corresponding author.**
E-mail address: *f.ahmadi@semnan.ac.ir*

Cite this article as:

Ahmadi Khatir,F. and Majidi, V., 2027. *Parametric Effects and Regression-Based Optimization of Drilling Performance in Glass Fiber-Reinforced Polymer Composites*. Mechanics of Advanced Composite Structures, 14(1), pp. xxx-xxx.

https://doi.org/10.22075/MACS.2025.39313.2050

1. Introduction

In the modern era, with the advancement of technology, composite materials have gained significant demand due to their broad spectrum of applications and superior properties compared to conventional materials. They are commonly employed in structural components. Among these composites, Glass Fiber Reinforced Polymer (GFRP) composites are particularly favored owing to their high strength-to-weight ratio, high fracture toughness, high specific elastic modulus, thermal resistance, excellent fatigue strength, and lightweight nature relative to traditional materials [1,2]. Owing to their exceptional and unique properties, these composites have established a prominent position in the automotive, aerospace, and marine industries. With the increasing demand for such composites, special attention has been devoted to their manufacturing and machining processes.

Machining of these composites differs significantly from conventional materials due to their heterogeneous and anisotropic characteristics. Among various machining operations performed on composites, drilling is one of the most common processes. Components fabricated from GFRP composites are typically manufactured near-net-shape and require holes for assembly purposes. Drilling is a critical operation since concentrated forces can induce severe damage to the composite structure [3]. Therefore, selecting appropriate process parameters during drilling is of paramount importance. Drilling of GFRP often leads to various damage modes, including matrix cracking, thermal degradation, fiber breakage, peeling, and delamination.

Babu and Philip [4] investigated the influence of spindle speed and feed rate on delamination behavior in composite materials through drilling experiments based on the Taguchi method, utilizing three different tools: twist drill, end mill, and core drill. Their results demonstrated that increasing spindle speed while decreasing feed rate could reduce delamination within the specified ranges of speed and feed. Chaudhari et al. [5] evaluated the effect of machining parameters—such as cutting speed, depth of cut, and feed rate—during composite drilling. They employed Adaptive Neuro-Fuzzy Inference System (ANFIS) models to predict the delamination factor and successfully identified optimal combinations of machining parameters. Velaga and Cadambi [6] studied and analyzed the influence of cutting parameters, including cutting speed and feed rate, during drilling under both experimental and numerical simulation conditions. Experimental and simulation results revealed delamination induced by drilling and confirmed reasonable agreement between experimental data and numerical simulations.

Prasad and Chaitanya [7] focused on the influence of cutting parameters and material properties on hole delamination and proposed optimal cutting conditions to minimize delamination and improve hole quality. Parameters such as spindle speed, feed rate, material thickness, and fiber orientation were examined. Their findings indicated that delamination is predominantly influenced by material thickness, followed by feed rate and fiber orientation. The influence of tool geometry on manufacturing performance has also been reported in metal forming processes, where different die patterns in rubber pad forming were shown to affect the forming behavior and quality of metallic bipolar plates [8]. Bilal et al. [9] investigated the drilling of glass fiber-reinforced composite tubes using different drill types at a constant spindle speed of 5000 rpm and six distinct feed rates. They demonstrated that drill geometry significantly affects drilling performance: a center-cut drill generates lower thrust forces, whereas a twist drill produces higher thrust forces. The severity of damage varies depending on tool geometry and feed rate [10]. Notably, at lower feed rates, a standard twist drill causes increased delamination and uncut fibers compared to other drill types, while the center-cut drill exhibits superior performance by inducing less damage.

Nayak et al. [11] conducted experiments to study delamination at the entry and exit sides of GFRP laminates as well as surface roughness. Cutting speed, feed rate, and drill diameter were considered as three input parameters at four different levels. They employed a desirability function approach to convert multiple responses into a single equivalent response and utilized regression analysis to develop a relationship between the composite desirability index and input parameters, resulting in a valid mathematical model. Finally, a simulated annealing algorithm was applied to obtain optimal parameter settings. Niranjan et al. [12] performed a review study aimed at minimizing composite delamination through appropriate drill tool selection. They examined various drill types—including twist drills, saw drills, step drills, candle drills, and dagger drills—and concluded that these tools play a crucial role in reducing delamination errors by controlling thrust force and matrix resistance. They further noted that conventional twist drills are prone to bending deformation and exceed interlaminar bonding, leading to delamination defects.

Niranjan et al. [13] analyzed the influence of three distinct drill types (fluted, twist, and brad types) and process parameters (feed rate and machining speed) on hole quality defects in composites. They employed the Technique for Order Preference by Similarity to Ideal Solution (TOPSIS) for multi-criteria optimization to minimize hole quality errors during drilling. Their results indicated that fluted-type drills at higher spindle speeds produce fewer defects in drilled holes. Anand et al. [14] provided a comprehensive review of challenges, recent experiences, and future aspects of mechanical micro-drilling of glass and carbon fiber-reinforced polymer composites. They examined chip removal mechanisms and compared them with conventional-scale technologies. Additionally, they discussed geometric defects arising from micro-drilling (such as delamination, burrs, and fiber protrusion) as well as cutting energy aspects.

Aveen et al. [15] investigated the influence of drilling factors on the quality of produced holes. They drilled holes in epoxy resin-based glass fiber composites reinforced with carbon nanotubes (CNTs) at filler contents of 0%, 1%, and 1.5%. Operational parameters, including spindle speed and feed rate, were varied during experiments. Thrust force and torque were measured using a digital drilling machine equipped with a dynamometer. A multi-output random regression model based on machine learning with hyperparameter tuning was employed to predict torque (T), thrust force (F), and the delamination factor. They found that spindle speed is the most influential parameter affecting delamination, followed by feed rate, and finally the filler content.

In addition to polymer matrix composites, research on metal matrix composites (MMCs) has also demonstrated similar machining challenges. Krishnamurthy et al. [16] and Palanikumar and Davim [17] investigated drilling of Al/SiC and Al/Al_2O_3 MMCs, respectively, highlighting the significant effects of cutting parameters on thrust force, torque, and surface quality. These studies underscore the universal nature of drilling challenges across different composite systems [18].

Recent advances in manufacturing process optimization have demonstrated the effectiveness of various computational intelligence approaches. Modanloo et al. [19] employed metaheuristic optimization algorithms and supervised machine learning techniques to model tensile strength and wear resistance in friction stir processed metal matrix composites, highlighting the superior performance of data-driven approaches under data-limited conditions. Elyasi and Modanloo [20] integrated finite element simulation with the reduced basis method for optimizing billet shape in cold forging processes, achieving significant reductions in forging force. Furthermore, Modanloo et al. [21] developed a novel Gradient Enhanced-Expert Informed Neural Network (GE-EINN) architecture for forming depth prediction, demonstrating substantial improvements in extrapolation scenarios compared to conventional machine learning models.

While these studies have successfully applied advanced optimization and modeling techniques to various manufacturing processes, the drilling of GFRP composites presents unique challenges that require specialized consideration. The novelty of the present work lies in several key aspects: (1) the simultaneous multi-response optimization of thrust force, torque, and delamination factor using the desirability function approach within the RSM framework; (2) the comprehensive experimental validation through confirmation tests conducted at the optimized conditions, ensuring the practical reliability of the predicted optimum; (3) the quantitative assessment of delamination using high-resolution digital image processing with systematic validation; and (4) the systematic investigation of the interactive effects of drilling parameters on multiple quality responses in GFRP composites. Unlike studies focusing on single-response optimization or purely computational approaches, this work provides a complete experimental-numerical framework validated through physical experiments, offering practical guidelines for industrial drilling of GFRP components.

Despite extensive efforts to develop equations that correlate drilling phenomena with influential parameters, a comprehensive and accurate model capable of fulfilling industrial requirements in machining has not yet been established. This limitation stems from the inherent complexity of the drilling process, necessitating extensive and widespread research to achieve a deeper understanding. Therefore, this study aims to investigate the influence of drilling parameters and propose a model for enhancing drilling quality in GFRP composites.

2. Experimental Procedure

2.1. Fabrication of Composite Specimens

A composite material consists of one or more discontinuous phases embedded within a continuous phase. The discontinuous phase is typically harder and stronger than the continuous phase; hence, it is referred to as the reinforcement. Reinforcements can exhibit various morphologies, including particulate, flake, fibrous, and platelet forms. The continuous phase is designated as the matrix. Fundamentally, a composite comprises three distinct regions: the matrix phase, the reinforcement phase, and the interfacial region between them, which collectively determine the composite's properties and behavior. Composites can be classified based on matrix type into three main categories: polymer matrix composites (PMCs), metal matrix composites (MMCs), and ceramic matrix composites (CMCs) [22].

The primary constituents of the composite specimens employed in this study are fibers and resin. In multilayer composites, multiple fiber types may be incorporated, resulting in hybrid composites. In the present work, a single matrix type was utilized to ensure adequate interlaminar adhesion.

Table 1. Mechanical Properties of E92125 Glass Fibers [23]

Property	Unit	Value
Density	g/cm^3	2.3
Young's modulus	Gpa	80
Tensile strength	Gpa	3.3
Elongation at break	%	4
Coefficient of thermal expansion	1×10^{-6} /°C	1.0
Price	$/kg	5

These woven fabrics may exist in either non-crimp or yarn-woven configurations. The fibers employed herein featured a satin weave architecture with an individual ply thickness of approximately 0.20 mm. The fabric utilized for composite panel fabrication is illustrated in Fig. 1.

The laminates were fabricated using hand lay-up followed by pressure consolidation at room temperature using a compression press (without external heating), and then cured at ambient temperature (22°C) for 24 hours. The specimens possessed planar dimensions of 200 × 200 mm with a nominal thickness of 2.2 mm. The reinforcing fibers were E-glass fabric (commercial code E92125, manufactured by Interglass), whose mechanical properties are presented in Table 1.

Fig. 1. Satin Weave Pattern of E-Glass Fabric Used in Composite Specimen Fabrication

The matrix resin was an epoxy system (Araldite LY 5052, Huntsman Corporation) cured with an amine-based hardener (HY 5052). This high-performance epoxy resin is predominantly employed in manufacturing components requiring superior mechanical properties, such as glider aircraft parts, automotive and marine structures (e.g., boats), and sporting goods. The resin exhibits a transparent liquid appearance with a density of 1.16–1.18 g/cm^3 at 25°C. The cured properties of LY 5052 resin are summarized in Table 2 [24].

Table 2. Cured Mechanical Properties of LY5052 Epoxy Resin [24]

Property	Unit	15 hours at 50°C	7 days at ambient temperature
Tensile strength	Gpa	82–86	49–71
Elongation at break	%	3.5–5.5	1.5–2.5
Tensile modulus	Gpa	3350–3350	3350–3550
Flexural strength	Gpa	126–128	<128
Flexural modulus	Gpa	2950–3000	<3000
Poisson's ratio	-	0.35	0.3
Fracture energy	J/m^3	20.2 ± 1.0	-

The composite shaping process adopted in this research was compression molding performed at ambient temperature. This technique utilizes a two-part mold, yielding specimens with smooth surfaces on both sides. The fabrication procedure combined compression molding with manual lay-up, wherein plies were stacked with a [0°/90°] fiber orientation. Following lay-up completion, the mold was cured at 22°C for 24 hours. The stacking sequence comprised ten alternating plies, resulting in a final laminate thickness of 2.2 ± 0.2 mm. The mechanical properties of the fabricated composite were characterized according to the ASTM D3039 standard. The prepared test specimen is shown in Fig. 2.

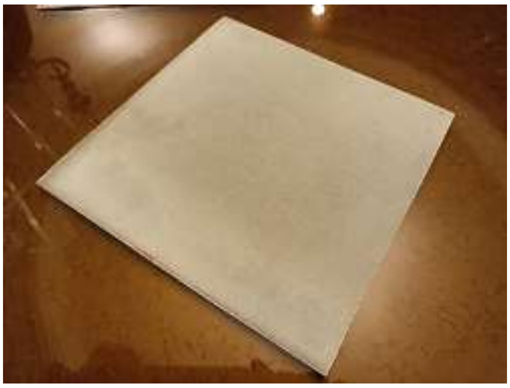

Fig. 2. Test Specimen of Glass Fiber-Reinforced Composite Plate

2.2. Mechanical Characterization of Fabricated Composite

The mechanical properties of the fabricated GFRP composite were characterized according to the ASTM D3039 standard for tensile testing of polymer matrix composite materials. Tensile tests were performed using a Universal Testing Machine (Zwick 250) with a 250 kN load cell.
Rectangular specimens with dimensions of 250 mm × 25 mm × 2.5 mm were prepared from separate composite laminates fabricated under identical conditions for tensile testing per ASTM D3039. To prevent grip-induced damage and ensure failure within the gauge section, reinforcement tabs with a length of 56 mm were bonded to both ends of each specimen using a high-strength adhesive.

Table 3. Mechanical properties of the fabricated GFRP composite (ASTM D3039).

Property	Value	Unit
Tensile Young's Modulus	25 ± 1	GPa
Ultimate Tensile Strength	320 ± 1	MPa
Elongation	3.2 ± 0.1	%
Poisson's Ratio	0.30 ± 0.02	-

All tests were conducted at a constant crosshead speed of 2 mm/min at room temperature (22°C). Five specimens were tested for each condition to ensure statistical reliability, and the results are reported as mean ± standard deviation. The measured mechanical properties of the fabricated GFRP composite are summarized in Table 3.

These experimentally determined properties were subsequently used as input material properties for the finite element analysis (FEA) performed in ANSYS, including the Poisson's ratio of 0.3 used in the modal analysis and the Von Mises failure criteria.

2.3. Drilling Fixture Design

Drilling of composite specimens requires a dedicated fixture capable of securely clamping the workpiece while simultaneously suppressing vibrations during machining. The designed fixture comprises two parallel plates—an upper plate and a lower base plate—featuring precisely aligned coaxial holes. The hole diameter in the upper plate was set to 5.2 mm, providing a slight clearance tolerance (approximately 0.2 mm) relative to the 5 mm drill bit diameter to facilitate smooth tool entry.

A critical design consideration was determining the optimal spacing between adjacent holes in the fixture. This spacing was optimized to minimize the influence of residual stresses induced by previously drilled holes on the thrust force and torque measurements of subsequent drilling operations, while also accommodating the dimensional constraints of the employed dynamometer table. To eliminate vibration transmission from the fixture to the dynamometer assembly, the fixture was rigidly mounted onto the dynamometer table using standard fasteners aligned with the table's threaded pattern. The dynamometer utilized in this study was a Kistler model 9255B three-component piezoelectric force dynamometer. Its mounting surface is perfectly flat, and the overall dynamometer configuration is illustrated in Fig. 3, with detailed dimensions provided in Fig. 4.

Fig. 3. Schematic Diagram of the Kistler Model 9255B Dynamometer

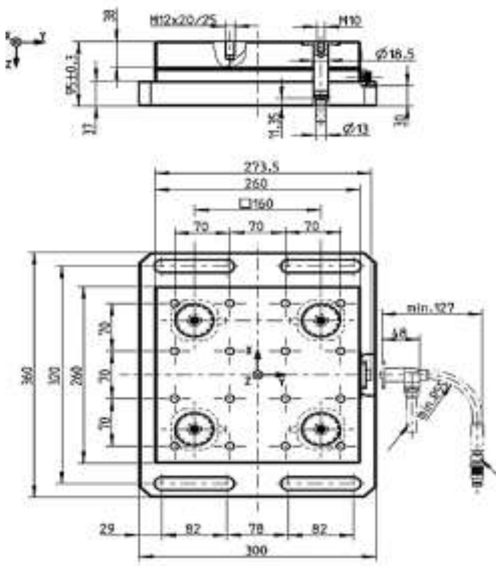

Fig. 4. Dimensional Specifications of the Kistler Model 9255B Dynamometer

To ensure that the fixture itself does not influence delamination damage while simultaneously providing effective plate damping and vibration suppression, the following design features were implemented [25]:

Lower plate holes: 26 mm diameter

Upper plate holes: two-step counterbore geometry consisting of:

A 5.2 mm diameter pilot hole (depth: 7 mm) to guide the drill bit

A 26 mm diameter clearance hole (depth: 8 mm) to allow chip evacuation and prevent interference with delamination at the exit side

The clearance hole diameter in the backing plate was designed to be 26 mm based on finite element analysis (FEA) performed in ANSYS. The drilling thrust force was experimentally measured using a dynamometer and found to be approximately 340 N. Using this force and the material properties (Poisson's ratio ≈ 0.3), modal analysis and Von Mises failure theory were applied to determine the stress-affected zone around the drilled hole. The simulation results indicated that the delamination and residual stress zone extends to approximately 25.5 mm in diameter. Therefore, a clearance hole diameter of 26 mm was selected to ensure that the entire damaged zone is fully contained within the clearance area, preventing any mechanical constraint from the backing plate. Additionally, the minimum distance between adjacent holes was set to 52 mm (2 × 26 mm) to prevent any interaction between stress fields of consecutive holes.

Mounting holes for secure attachment to the dynamometer were incorporated into the lower plate based on the dimensional specifications shown in Fig. 4. Detailed geometric features of the fixture, along with the configuration of the upper and lower plates, are presented in Fig. 5.

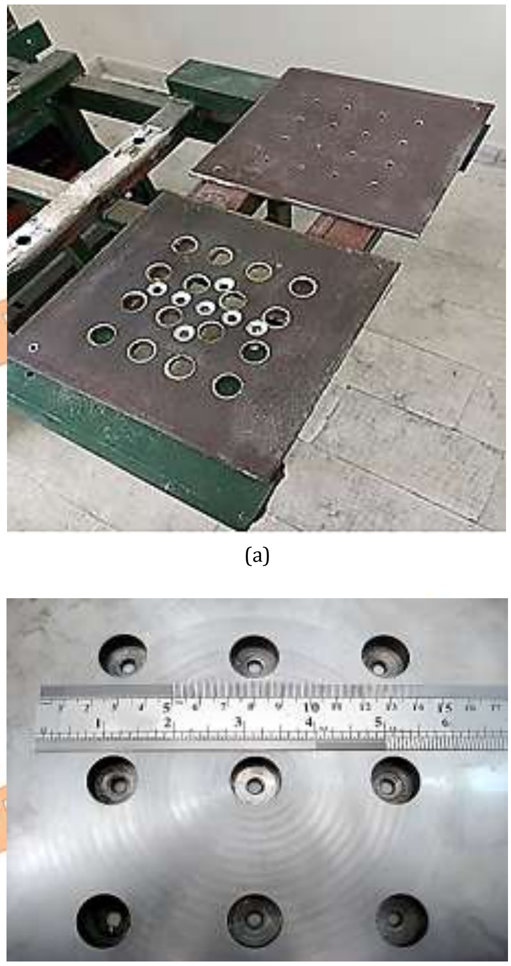

(a)

(b)

Fig. 5. (a) Drilled holes on fixture plates; (b) Detailed view of the upper fixture plate

2.4. *Drilling Tools*

The drill bits employed in this experimental study were manufactured from 5% cobalt high-speed steel (HSS-Co 5%) by Kuffler, a reputable German cutting tool manufacturer. All drills featured a nominal diameter of precisely 5 mm. The experimental matrix included variations in drill point angle, ranging from 90° to 130° in incremental steps. Detailed geometric specifications of the drill bits used in this investigation are illustrated in Fig. 6.

Fig. 6. 5 mm Diameter Drill Bits with Varying Point Angles

2.5. Experimental Design

Cutting parameters in the drilling process—specifically cutting speed and feed rate—significantly influence drilling thrust force and torque, thereby affecting the quality of the produced holes. The phenomena affected during drilling typically include surface roughness, delamination, machining forces (axial, radial, and tangential components), drilling-induced torque, metallurgical alterations at the machined surface, among others. The parameters influencing these phenomena (machining variables) can be categorized into four main groups:

(a) Machine setting parameters: cutting speed and feed rate

(b) Tool-related parameters: tool geometry (point angle and diameter), tool material, coating, and tool type based on external geometry

(c) Workpiece-related parameters: workpiece hardness, fiber volume fraction, fiber orientation, fiber stacking sequence, and workpiece thickness

(d) Process-related parameters: presence or absence of backing support during drilling

In this investigation, the primary objective was to evaluate the influence of machine setting parameters and drill point angle. Therefore, other influential variables were either eliminated or minimized. Since all test specimens were fabricated from identical composite materials—with uniform manufacturing processes including fiber type, resin system, lay-up sequence, curing time, and laminate thickness—the effects of variables other than cutting speed, feed rate, and drill point angle were considered negligible.

Furthermore, all drills shared identical material composition (HSS-Co 5%), diameter (5 mm), and external geometry. To eliminate the influence of tool wear, each drill was replaced after drilling five holes. All drilling operations were performed using the same dedicated fixture described in Section 2.2, which substantially minimized the effects of variables categorized under groups (c) and (d).

Consequently, three independent variables were selected for investigation: rotational speed (spindle speed), feed rate, and drill point angle. The experimental design was conducted using Design-Expert® software (Stat-Ease, Inc.). As summarized in Table 4, each parameter was examined at three discrete levels, with the corresponding factor levels explicitly defined.

Table 4. Experimental Design Parameters and Levels

Parameter	Symbol	Level 1	Level 2	Level 3
Spindle speed (rpm)	s	500	750	1000
Feed rate (mm/rev)	f	0.05	0.125	0.2
Drill point angle (°)	α	90	110	130

For each experimental run, drilling forces and torque were recorded in real-time by the Kistler dynamometer (model 9255B) and presented as time-series plots along the x, y, and z axes. Following the completion of drilling operations according to the experimental matrix, the induced damage was evaluated both qualitatively and quantitatively. Quantitative assessment of delamination at both entry and exit sides of each hole was performed on the upper and lower laminate surfaces using a high-resolution digital scanner. An appropriate grayscale threshold was determined through histogram analysis and pixel-by-pixel comparison between processed images and the original scanned images, as illustrated in Fig. 7. Based on the resulting binary images, the drilling-induced delamination factor was calculated as the ratio of the delaminated area (A_d) to the nominal hole area (A) [37]. The delamination factor (Fd) is mathematically expressed as:

$$F_d = A_d/A \quad (1)$$

In this study, the area-based delamination factor ($F_d = A_d/A_0$) was selected as the primary damage metric over the conventional diameter-based method ($F_{dmax} = D_{max}/D$) for several scientifically grounded reasons:

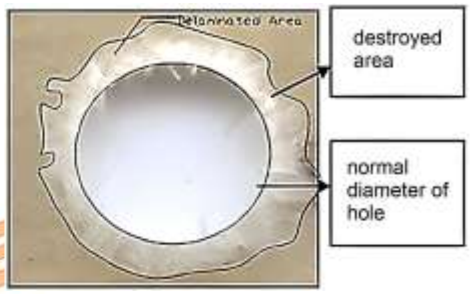

Fig. 7. Schematic Illustration of Delamination Factor Determination via Digital Image Processing [37]

First, in GFRP composites, the delamination zone at the drill exit typically exhibits irregular, non-circular shapes due to the anisotropic and heterogeneous nature of the material, fiber orientation effects, and non-uniform thrust force distribution. The diameter-based method, which considers only the maximum diameter, fails to capture this geometric complexity and may provide an incomplete representation of the actual damage extent.

Second, delamination in fiber-reinforced composites is fundamentally an energy-driven phenomenon. The delaminated area is directly correlated with the fracture energy absorbed during crack propagation, making it a more physically meaningful indicator of damage severity compared to a one-dimensional diameter measurement.

Third, the area-based method offers higher sensitivity to variations in drilling parameters, which is essential for accurate Response Surface Methodology (RSM) modeling. This enhanced sensitivity contributes to the high coefficient of determination ($R^2 > 0.90$) achieved in the regression analysis.

The delaminated areas were precisely quantified using digital image analysis. High-resolution images of the drill exit were captured using a scanner/digital microscope, and the delamination area was measured using ImageJ software (National Institutes of Health, USA). This approach provides objective, reproducible, and highly accurate measurements.

The area-based delamination factor has been widely validated in previous studies on drilling of composite materials, including the works of Davim and Reis [26], Tsao and Hocheng [27], Khashaba et al. [28], and Palanikumar [29], confirming its reliability and comprehensiveness for damage assessment in fiber-reinforced composites.

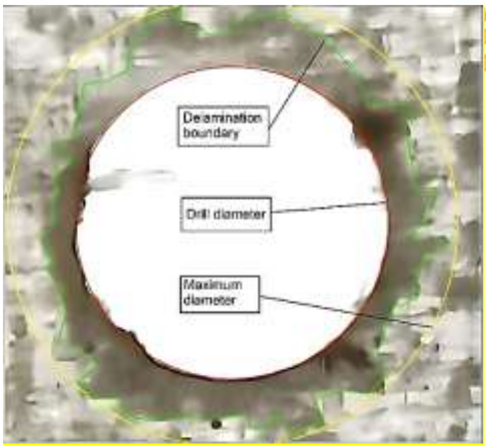

Fig. 8. Representative high-resolution scanned image of the drill exit for Run 10, illustrating the digital image processing methodology. The red circle indicates the nominal drill diameter (D = 5 mm), the green contour represents the actual delamination boundary detected by ImageJ, and the yellow circle denotes the maximum delamination diameter (Dmax). The irregular shape of the green contour clearly justifies the use of the area-based delamination factor (Fd = Ad/A) over the conventional diameter-based method.

3. Experimental Testing

To conduct the drilling experiments, the dynamometer was mounted onto a CNC machining center and securely fastened to the machine table using dedicated mounting fixtures. Data acquisition connections between the dynamometer and the host computer running the data acquisition software were established. The lower drilling fixture was then positioned on the dynamometer surface and rigidly clamped using the corresponding fasteners. The sequential setup stages are illustrated in Fig. 9.

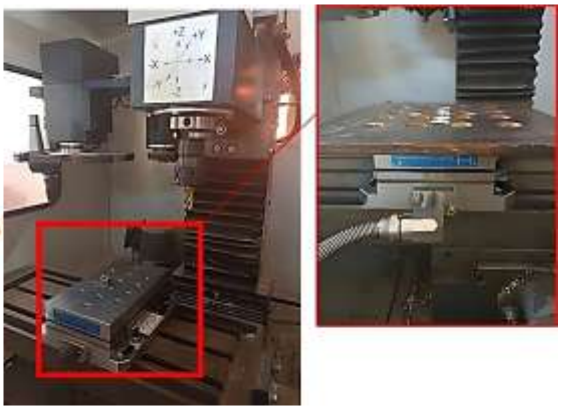

Fig. 9. Sequential Assembly of the Dynamometer onto the Milling Machine and Mounting of the Lower Drilling Fixture Plate

Subsequently, the composite laminate was placed onto the lower fixture plate, followed by positioning the upper fixture plate and securing the entire assembly through bolted connections. The assembly sequence is depicted in Fig. 10.

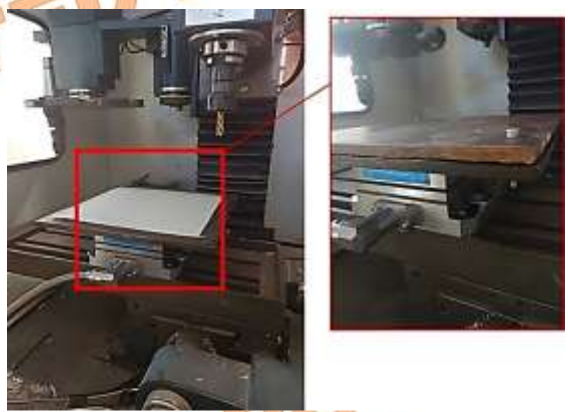

Fig. 10. Clamping of Composite Specimen Between Upper and Lower Fixture Plates Using Fastening Bolts

In the next stage, the machining center was configured according to the experimental parameters defined in the design matrix (Table 5), and the drilling operations were executed accordingly. Force and torque data were continuously recorded throughout each drilling cycle, and the corresponding time-series plots were extracted for analysis. The delamination factor for each drilled hole was calculated by scanning the hole region and determining the ratio of the damaged (delaminated) area to the nominal hole area, in accordance with Equation (1). Upon completion of delamination assessment and extraction of thrust force and torque values for each hole, the complete output dataset was compiled. These experimental results were subsequently entered into Table 5 to facilitate statistical analysis and interpretation of findings.

Table 5. Experimental Design and Output Results

Run	Spindle Speed (rpm)	Feed Rate (mm/rev)	Drill Point Angle (°)	Thrust Force (N)	Torque (N.cm)	Delamination Factor
1	750	0.125	110	229.1	5.4	1.37
2	750	0.200	130	305	12.4	1.55
3	500	0.125	130	159.4	10.5	1.33
4	500	0.125	90	156.4	10.9	1.45
5	1000	0.125	130	130.3	7.7	1.45
6	500	0.200	110	338.7	18.3	1.59
7	750	0.125	110	231.9	3.4	1.35
8	1000	0.050	110	93.8	6.0	1.08
9	750	0.125	110	237.6	3.5	1.37
10	750	0.050	130	83.5	10	1.30
11	1000	0.200	110	275.6	16.7	1.57
12	750	0.125	110	228.4	5.4	1.37
13	500	0.050	110	119.5	7.5	1.17
14	750	0.200	90	257.7	13.4	1.56
15	1000	0.125	90	114.3	15.4	1.33
16	750	0.125	110	241.5	9.0	1.37
17	750	0.050	90	95.0	2.1	1.10

3.1. *Experimental Procedure and Data Acquisition*

The selection of machining parameter ranges was guided by four key considerations: industrial practice, machine tool limitations, tool manufacturer recommendations, and literature findings. First, from an industrial perspective, the thin GFRP/epoxy laminate (2.2 mm thickness) is highly susceptible to peel-up and push-out delamination during drilling. The feed rate levels (0.05, 0.125, and 0.2 mm/rev) were selected to span the critical thrust force region associated with delamination onset in thin composite structures [30, 31].

Second, the spindle speed range was constrained by the operational capabilities of the CNC machining center. Speeds above 1000 rpm could induce excessive vibrations and chatter in thin laminates, while lower speeds were avoided to prevent excessive thrust forces.

Third, the baseline ranges were established according to the technical specifications provided by Kofler Gesenkschmiede GmbH (Austria) [36] for their 5% HSS-Co solid drills [32]. HSS-Co drills were preferred due to their superior toughness, which prevents edge chipping during the intermittent cutting of fiber-reinforced composites [33].

Fourth, preliminary trial experiments and literature recommendations [33–35] further refined these ranges. At spindle speeds below 500 rpm, excessive thrust forces led to severe fiber pull-out and matrix cracking at the hole entry. Conversely, speeds above 1000 rpm risked thermal degradation of the epoxy matrix. Three drill point angles (90°, 110°, and 130°) were selected to systematically investigate the influence of tool geometry on delamination mechanisms [34, 35].

The experimental design was developed using the Box-Behnken Design (BBD) under the Response Surface Methodology (RSM) framework to investigate the effects of three drilling parameters on the response variables (thrust force, torque, and delamination factor). The BBD was selected for its efficiency in requiring fewer experimental runs while maintaining good prediction accuracy.

Three drilling parameters were considered as input variables, each at three levels:

Spindle speed (N): 500, 750, and 1000 rpm

Feed rate (f): 0.05, 0.125, and 0.2 mm/rev

The BBD consists of 17 experimental runs, including:

12 edge center points (midpoints of the cube edges)

5 center points (to estimate pure error and verify model adequacy)

The design matrix with coded and actual values of the process parameters is presented in Table 5. The experiments were randomized to minimize the effects of uncontrolled variability and ensure that the observations are independent.

The experimental design and subsequent statistical analysis were performed using Design-Expert software (Version 13, Stat-Ease Inc., Minneapolis, MN, USA). A second-order polynomial model was fitted to the experimental data to establish the relationship between the input parameters and the response variables.

All 17 experimental runs were conducted in random order as automatically generated by the Design-Expert software to minimize the effects of uncontrolled variables (such as environmental temperature fluctuations, humidity changes, tool wear progression, and measurement drift) and to ensure the statistical validity of the results.

Each experimental condition was replicated three times (n=3) to ensure statistical reliability and to enable the calculation of standard deviations. The 5 center points included in the Box-Behnken Design matrix were strategically placed by the software to estimate pure error and verify model adequacy. All reported values in this study represent the arithmetic mean of the three replicates, with standard deviations calculated for each measurement to indicate the variability and reliability of the experimental data. The small standard deviations observed (typically less than 5% of the mean values) confirm the high repeatability and consistency of the experimental setup and measurement procedures.

4. Analysis of Experimental Results

Prior to initiating the optimization process within the software environment, the adequacy of the developed regression models was rigorously evaluated for all three response parameters. Model validation was performed through statistical analysis of the Analysis of Variance (ANOVA) tables generated for each response variable. Key diagnostic indicators—including the p-value associated with the model terms and the Lack of Fit test—were examined to assess statistical significance and model fitness.

Additionally, the Fit Statistics section provided by the software reports critical metrics such as the Adjusted R^2 and Predicted R^2 values, which quantify the model's predictive capability and its ability to explain the variability in the experimental data. Higher values of these coefficients (approaching unity) indicate superior model performance and reliability.

The comprehensive statistical validation results for all three response variables—drilling torque, thrust force, and delamination factor—are summarized in Table 6. The analysis confirmed that the developed models exhibit statistically significant terms (p-value < 0.05), non-significant Lack of Fit (p-value > 0.05), and strong correlation between predicted and actual values (Adjusted R^2 and Predicted R^2 > 0.90), thereby validating their suitability for subsequent optimization and parametric analysis.

Table 6 summarizes the statistical validation results from ANOVA and model fit statistics for the three response variables. The p-values indicate the statistical significance of model terms ($p < 0.05$), while non-significant Lack of Fit ($p > 0.05$) confirms adequate model fit. Adjusted R^2 and Predicted R^2 values demonstrate the model's predictive capability.

4.1. Drilling Torque Analysis

To evaluate the statistical significance of input parameters and validate the experimental design results, Analysis of Variance (ANOVA) was performed on the drilling torque dataset. As presented in Table 6, the ANOVA results confirm that the developed statistical model is statistically significant and adequately describes the torque response behavior across the investigated parameter ranges. A p-value less than 0.05 for the main effects indicates that these parameters exert a statistically significant influence on drilling torque. Consequently, with statistical validation of the model established, subsequent analysis of process parameter effects on drilling torque is considered reliable and credible.

Drilling torque represents one of the most critical mechanical parameters in the drilling process, directly influenced by cutting conditions and tool geometry. Examination of torque variations provides valuable insight into chip formation mechanisms, shear force magnitudes, and ultimately the overall quality of the drilling operation.

Table 6. ANOVA and Fit Statistics for Response Models

Response	P-Value	Lack of Fit	Adjusted R^2	Predicted R^2
Torque	< 0.0001	0.6274	0.8739	0.8987
Thrust Force	< 0.0001	0.5945	0.9955	0.9871
Delamination Factor	< 0.0001	0.3016	0.9929	0.9821

The first plot, illustrated in Fig. 11(a), demonstrates the effect of spindle speed on drilling torque. According to the experimental results, torque values increase at low spindle speeds. This behavior can be attributed to elevated friction between the tool and workpiece, chip adhesion to cutting edges, and unstable cutting conditions within this speed range. As spindle speed increases up to approximately 750 rpm, torque exhibits a decreasing trend, which can be associated with improved cutting conditions, reduced shear stress, and facilitated chip formation and evacuation. However, beyond this threshold, torque increases again at higher spindle speeds, likely due to elevated cutting zone temperature, intensified tool wear, and increased friction between the drill flute and hole wall. These results indicate that drilling torque exhibits a nonlinear relationship with spindle speed, with a discernible optimal speed range for minimizing torque.

The second plot, presented in Fig. 11(b), illustrates the influence of feed rate on drilling torque. The results demonstrate that torque increases monotonically with increasing feed rate. This behavior is primarily attributed to the increased undeformed chip thickness and cross-sectional area, leading to greater material removal volume per unit time and consequently higher shear forces and required drilling torque. Additionally, elevated feed rates may increase tool-workpiece contact pressure and reduce process stability, both contributing to torque elevation.

Finally, the effect of drill point angle on drilling torque is examined in Fig. 11(c). The results indicate that torque decreases with increasing drill point angle. This reduction stems from alterations in the cutting zone geometry and decreased cross-sectional area of the undeformed chip. More precisely, as the point angle increases, the actual chip width approaches the nominal chip width, resulting in more uniform stress distribution along the cutting edges. This phenomenon reduces material resistance to shearing and consequently decreases the required drilling torque.

Figure 12 illustrates the two-way interaction effects of the three input variables on drilling torque. As shown in Fig. 12(a), which depicts the simultaneous influence of spindle speed and feed rate on torque at a constant drill point angle, torque increases monotonically with rising feed rate. In contrast, torque does not exhibit a consistent trend with increasing spindle speed—instead, it follows a nonlinear pattern characterized by an initial decrease followed by a subsequent increase. This behavior is directly correlated with variations in the undeformed chip width during the drilling process.

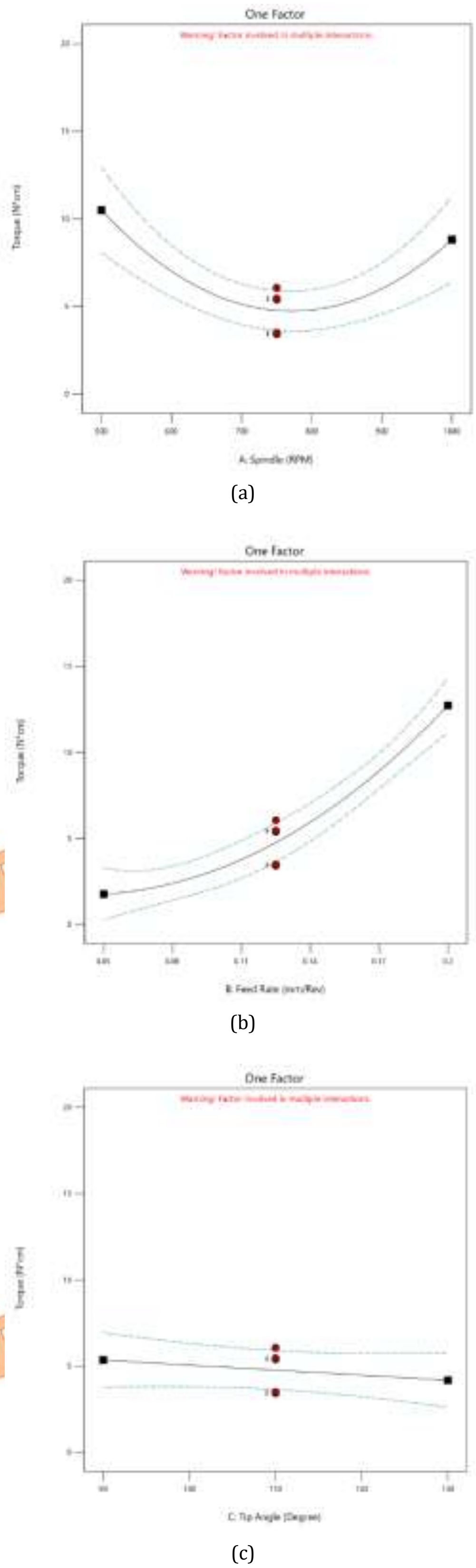

Fig. 11. Effect of (a) spindle speed, (b) feed rate, and (c) drill point angle on drilling torque

Figure 12(b) presents the combined effect of spindle speed and drill point angle on torque. The results indicate that any increase in drill point angle leads to a reduction in drilling torque. Meanwhile, variations in spindle speed demonstrate no pronounced or systematic influence on torque magnitude within the investigated range. Generally speaking, regarding drilling torque, any factor that increases the undeformed chip width during the drilling operation will consequently elevate the required torque. This principle underlies the observed trends across all interaction plots.

Figure 12(c) displays the interaction between feed rate and drill point angle. Consistent with previous observations, torque increases with higher feed rates, while larger drill point angles result in reduced torque values. This opposing influence confirms that feed rate and drill point angle act as counterbalancing parameters in torque control. Equation (2) presents the regression model developed for predicting drilling torque as a function of the input parameters:

$$
\begin{aligned}
Torque = {} & +51.27643 - 0.095366s \\
& - 2.17222\, f \\
& - 0.207950\, \alpha \\
& - 0.000379 s\alpha \\
& + 0.000091 s^2
\end{aligned}
\quad (2)
$$

Where:
s = spindle speed (rpm)
f = feed rate (mm/rev)
α = drill point angle (°)

Analysis of the torque prediction model reveals that feed rate exerts the most dominant influence on drilling torque among all input variables. Consequently, for effective control of the drilling process, feed rate should be prioritized as the primary controllable parameter, followed by drill point angle selection. Spindle speed, while exhibiting a secondary nonlinear effect, plays a comparatively lesser role in direct torque regulation.

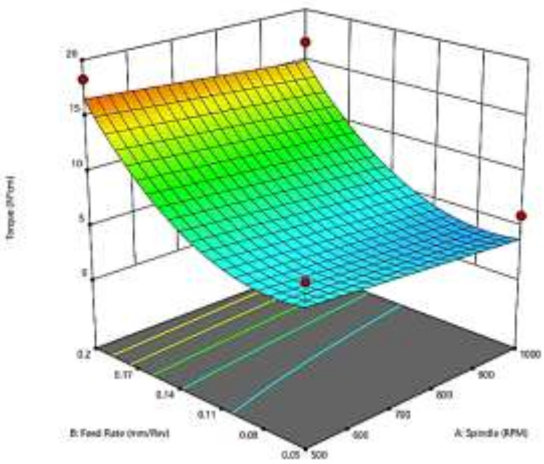

(a)

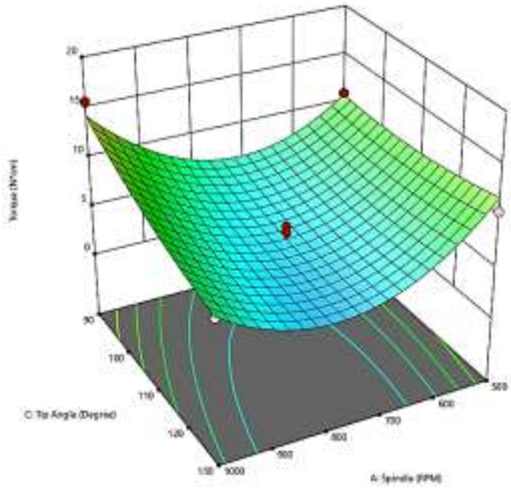

(b)

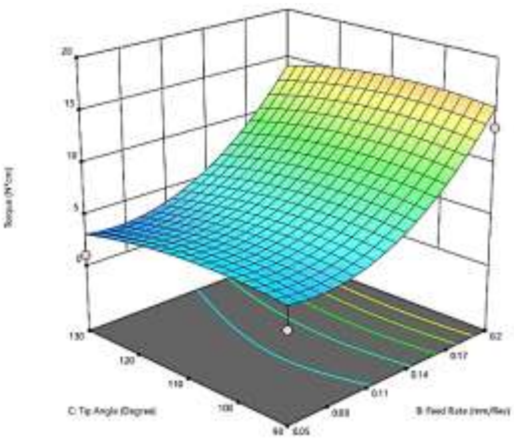

(c)

Fig. 12. Interaction effects of (a) spindle speed and feed rate, (b) spindle speed and drill point angle, and (c) feed rate and drill point angle on drilling torque

4.2. Drilling Thrust Force Analysis

The effect of spindle speed on drilling thrust force is illustrated in Fig. 13(a). Generally, thrust force decreases with increasing spindle speed. This reduction can be attributed to the diminished undeformed chip thickness at higher rotational speeds, which lowers the material resistance encountered by the drill's chisel edge and cutting lips during penetration.

Figure 13(b) presents the influence of feed rate on thrust force. The results demonstrate that thrust force increases monotonically with rising feed rate. This behavior stems from the increased undeformed chip thickness and cross-sectional area of material being removed per revolution, resulting in higher axial resistance and consequently elevated thrust forces.

Finally, the effect of drill point angle on thrust force is examined in Fig. 13(c). The experimental results indicate that thrust force exhibits minimal sensitivity to variations in drill point angle. Specifically, thrust force initially shows a slight increase followed by a gradual decrease as the point angle increases. This non-monotonic behavior suggests that the influence of point angle on thrust force is secondary compared to spindle speed and feed rate, as the axial force component is predominantly governed by the drill's chisel edge geometry and feed-induced chip load rather than the peripheral cutting edge angle.

Figure 13 illustrates the two-way interaction effects of the three input variables on drilling thrust force.

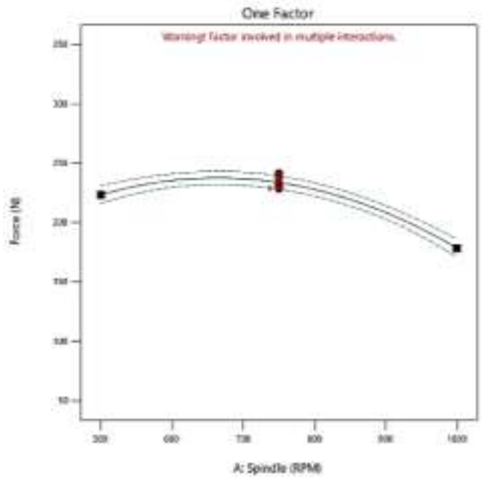

(a)

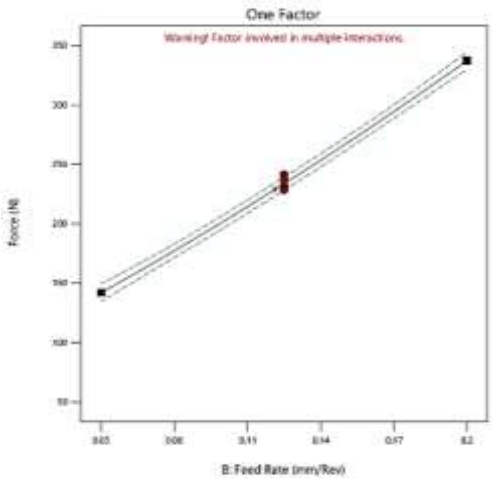

(b)

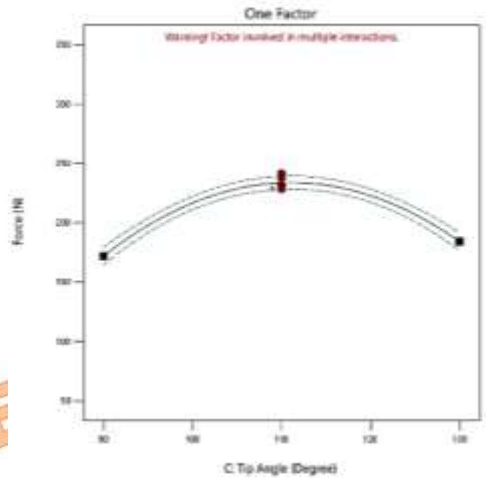

(c)

Fig. 13. Effect of (a) spindle speed, (b) feed rate, and (c) drill point angle on drilling thrust force

As shown in Fig. 14(a), which depicts the simultaneous influence of spindle speed and feed rate on thrust force, the force increases monotonically with rising feed rate. Conversely, thrust force exhibits a nonlinear trend with increasing spindle speed—initially decreasing and subsequently increasing beyond a certain threshold. This behavior can be attributed to competing mechanisms: at moderate speeds, reduced chip thickness lowers cutting resistance, whereas at higher speeds, elevated temperatures and increased friction between the drill flute and hole wall counteract this effect.

Figure 14(b) presents the combined effect of spindle speed and drill point angle on thrust force. The contour plot reveals a non-monotonic response, where thrust force initially increases and then decreases with variations in both parameters. This complex behavior stems from alterations in the effective undeformed chip thickness and stress distribution along the cutting edges as the geometric and kinematic conditions evolve during drilling.

Figure 14(c) displays the interaction between feed rate and drill point angle. Consistent with the main effects analysis, thrust force increases significantly with higher feed rates. In contrast, drill point angle demonstrates minimal influence on thrust force magnitude, confirming that this parameter plays a secondary role in axial force generation compared to kinematic parameters.

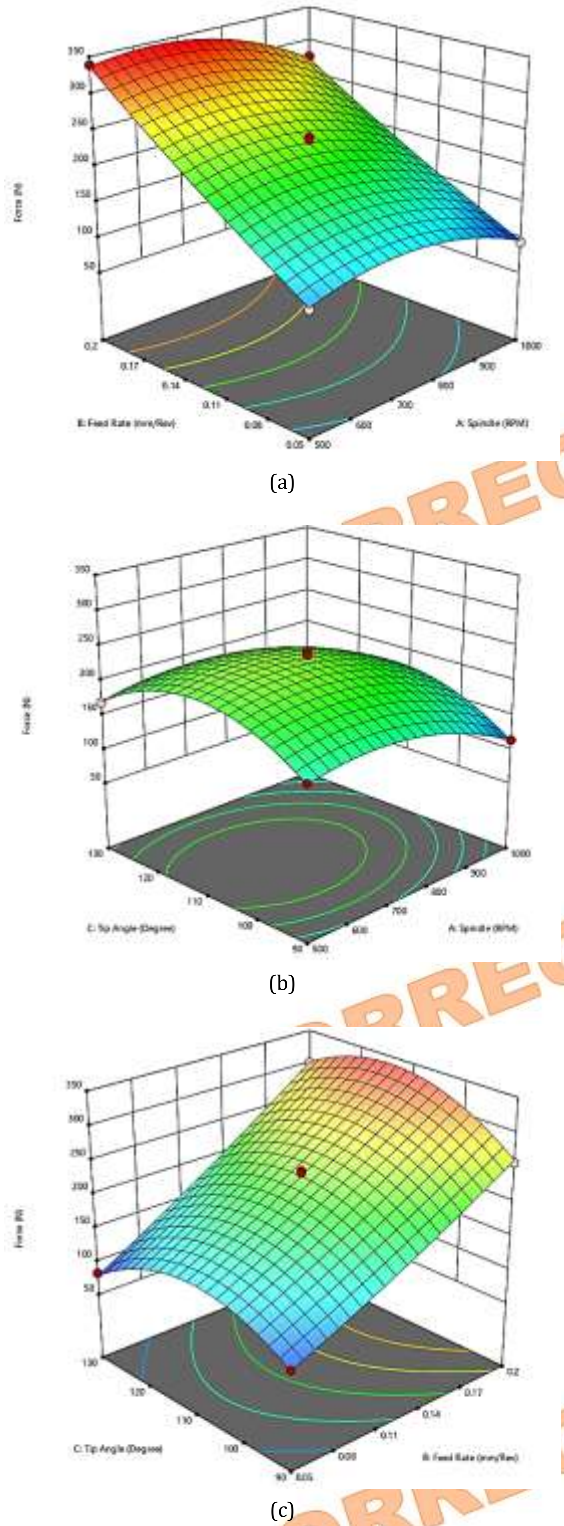

Fig. 14. Interaction effects of (a) spindle speed and feed rate, (b) spindle speed and drill point angle, and (c) feed rate and drill point angle on drilling thrust force

Equation (3) presents the regression model developed for predicting drilling thrust force:

$$Force = -1729.38252 + 0.688837s + 398.68415f + 29.36809\alpha - 0.500137sf + 0.000645s\alpha + 9.19637f\alpha - 0.000525s^2 + 1070.38458f^2 - 0.139514\alpha^2 \quad (3)$$

Statistical analysis of the thrust force model reveals the following hierarchy of parameter significance:

Feed rate exerts the most dominant influence on thrust force

Drill point angle exhibits a secondary, moderate effect

Spindle speed demonstrates the least direct influence (though its nonlinear interaction effects remain noteworthy)

Consequently, for effective control of thrust force during GFRP drilling operations, feed rate should be prioritized as the primary adjustable parameter, followed by drill point angle selection. Spindle speed optimization should be considered primarily for its indirect effects on heat generation and surface integrity rather than direct thrust force regulation.

4.3. Delamination Analysis

Delamination is recognized as the most prevalent defect generated during drilling of glass fiber-reinforced polymer (GFRP) composites. This phenomenon weakens the material surrounding the hole perimeter, thereby rendering the component susceptible to severe damage propagation and structural strength degradation. Consequently, delamination assessment holds paramount importance in composite drilling operations, as thrust force and torque directly govern the initiation and propagation of interlaminar separation.

The primary objective of this research is to identify optimal drilling parameters that minimize the delamination factor. Figure 15(a) presents the effect of spindle speed on the delamination factor. According to the experimental results, delamination decreases progressively with increasing spindle speed. This reduction is substantial and can be attributed to diminished radial cutting forces acting on the composite layers at higher rotational velocities, thereby reducing interlaminar stress concentrations that trigger delamination.

Figure 15(b) illustrates the influence of feed rate on delamination severity. The results demonstrate that delamination increases markedly with elevated feed rates. The primary mechanism underlying this behavior is the increased ratio of undeformed chip width to nominal chip width, which generates higher compressive stresses at the hole exit zone. These elevated stresses exceed the interlaminar bonding strength, leading to intensified delamination damage.

Figure 15(c) displays the effect of drill point angle on delamination. The influence of point angle on delamination is relatively marginal compared to kinematic parameters; however, a mild increasing trend in delamination is observed with larger point angles. This increment can be ascribed to the increased effective cutting width at higher point angles, which elevates the radial force component acting perpendicular to the fiber-matrix interface and consequently promotes interlaminar separation.

Figure 15 illustrates the two-way interaction effects of input parameters on the delamination factor during drilling operations.

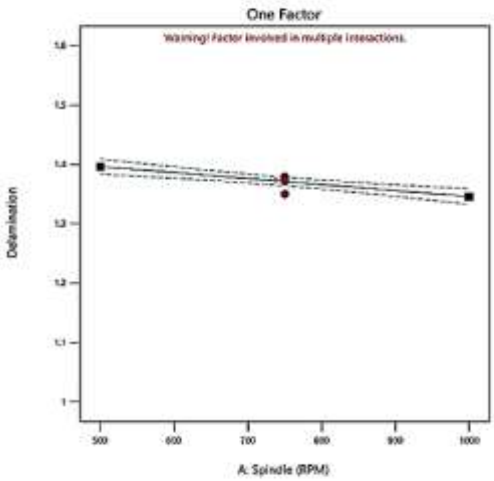

(a)

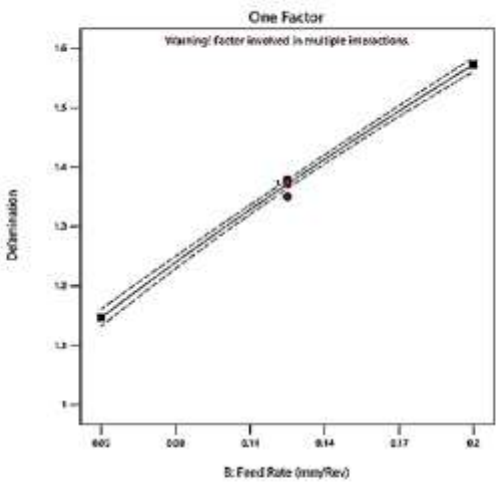

(b)

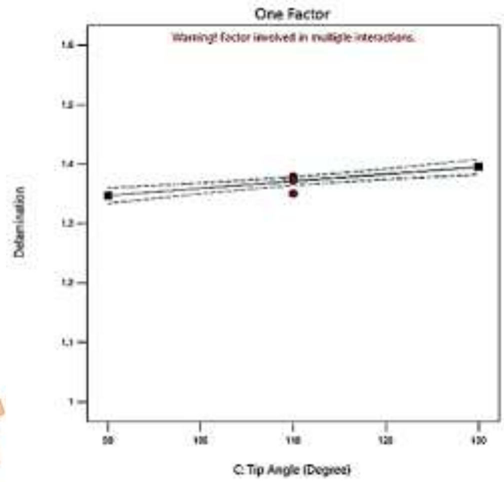

(c)

Fig. 15. Effect of (a) spindle speed, (b) feed rate, and (c) drill point angle on delamination factor

. Figure 16(a) presents the simultaneous influence of spindle speed (S) and feed rate (f) on delamination severity. Consistent with previous findings, increasing spindle speed leads to reduced delamination and improved hole quality. Conversely, elevated feed rates exert an adverse effect, intensifying delamination defects due to increased compressive stresses at the hole exit.

Figure 16(b) examines the combined effect of spindle speed and drill point angle (α) on delamination. The results indicate that spindle speed demonstrates a more pronounced influence on delamination formation compared to drill point angle. Nevertheless, it should be noted that the effects of both parameters remain relatively marginal when compared to feed rate, which plays the dominant role in delamination initiation and propagation.

Figure 16(c) displays the interaction between feed rate and drill point angle. The results reveal that increases in either parameter lead to elevated delamination levels. The pronounced delamination observed at high feed rates can be attributed to the dominance of the thrust-induced penetration mechanism: as feed rate increases, the deformed chip thickness becomes substantially smaller than its nominal value, resulting in elevated compressive forces at the hole exit zone that exceed interlaminar bonding strength. Regarding drill point angle, the increased cutting width associated with larger point angles generates higher radial forces acting perpendicular to the fiber-matrix interface. These radial forces directly contribute to the initiation and propagation of interlaminar separation.

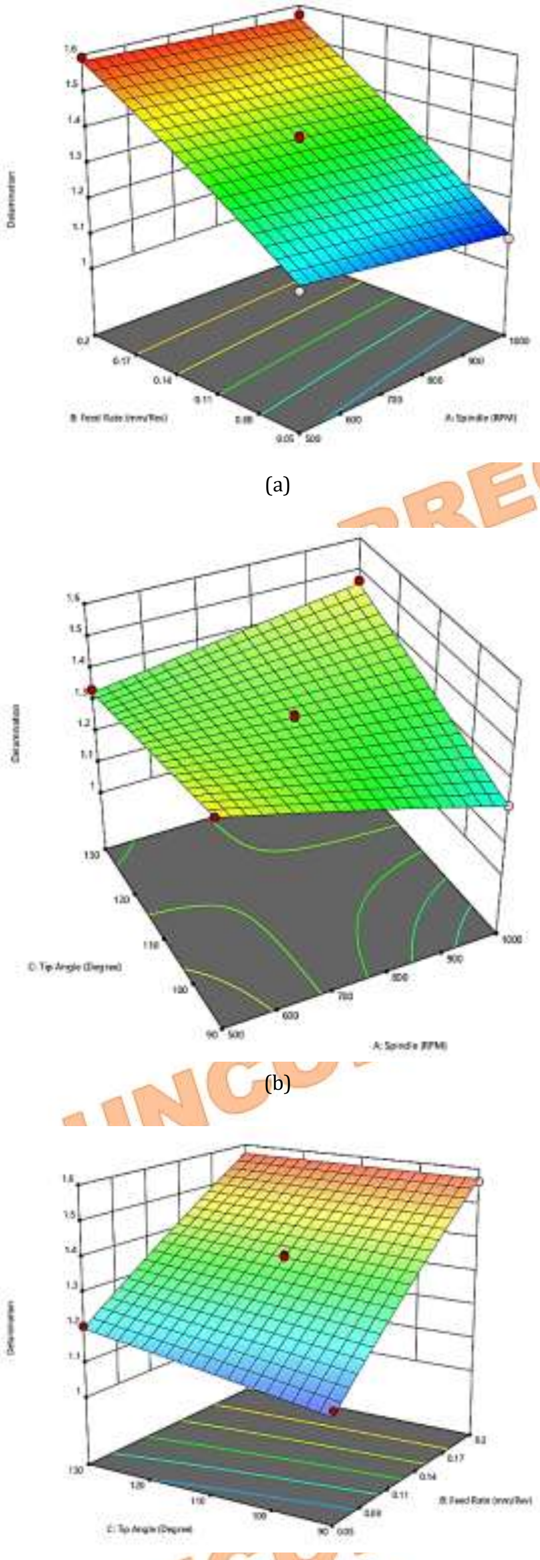

(a) (b) (c)

Fig. 16. Interaction effects of (a) spindle speed and feed rate, (b) spindle speed and drill point angle, and (c) feed rate and drill point angle on delamination factor

Equation (4) presents the regression model developed for predicting the delamination factor (Fd):

$$F_d = +3.74395 - 0.004679s + 8.38426f - 0.022485\alpha + 0.001569sf + 0.000039s\alpha - 0.032494f\alpha \quad (4)$$

Statistical analysis of the delamination prediction model reveals the following hierarchy of parameter significance:

Feed rate (f) exerts the most dominant influence on delamination (coefficient: +8.38426)

Drill point angle (α) exhibits a secondary effect (coefficient: −0.022485)

Spindle speed (S) demonstrates the least direct influence (coefficient: −0.004679)

Consequently, to minimize delamination during GFRP drilling operations, feed rate should be prioritized as the primary controllable parameter, followed by drill point angle selection. Spindle speed optimization, while beneficial for reducing delamination, plays a comparatively secondary role in defect control.

5. Discussion

5.1. Delamination Mechanisms: Peel-up vs. Push-out

Delamination in drilled composite laminates occurs through two distinct mechanisms: peel-up at the entry side and push-out at the exit side [30].

Peel-up delamination is primarily driven by torque-induced peeling moments. As the drill bit rotates and engages with the top plies, the tangential cutting forces create a moment that lifts the entry plies upward, causing interlaminar separation. The severity of peel-up delamination is mainly influenced by:

Torque magnitude: Higher torque increases the peeling moment

Spindle speed: Higher speeds typically reduce torque, thereby decreasing peel-up

Feed rate: Higher feed rates increase torque, promoting peel-up

Drill geometry: Helix angle and point angle affect the cutting force distribution

Push-out delamination, on the other hand, is driven by thrust force-induced bending stresses. As the drill approaches the exit surface, the thrust force causes the remaining uncut plies to bend downward. When the bending stress exceeds the interlaminar strength, delamination occurs. The key factors affecting push-out delamination include:

Thrust force magnitude: Higher thrust force increases bending stresses

Uncut chip thickness: As the drill approaches the exit, the decreasing thickness reduces bending stiffness

Feed rate: Higher feed rates increase thrust force, promoting push-out

Spindle speed: Higher speeds reduce thrust force, decreasing push-out

Drill diameter: Larger diameters generate higher thrust forces

According to established literature [28, 37], push-out delamination is typically 2-3 times more severe than peel-up delamination in GFRP composites. This is because:

The critical thrust force required to initiate push-out is lower than the critical torque for peel-up

The bending stiffness of the uncut plies decreases significantly as the drill approaches the exit

Push-out delamination has a greater impact on the structural integrity and load-bearing capacity of bolted joints

In this study, we focused on exit delamination (push-out mechanism) as it represents the more critical damage mode for structural applications.

The experimental results clearly demonstrate that increasing spindle speed reduces both thrust force and delamination factor, while increasing feed rate has the opposite effect, which is fully consistent with the push-out delamination mechanism described in the literature[30,37].

5.2. Confirmation Experiments

To validate the predictive capability of the developed regression models and verify the practical utility of the optimization results, confirmation experiments were conducted at the optimized drilling conditions identified through the multi-response optimization using the desirability function approach (Drill point angle: 110°, Spindle speed: 720 rpm, Feed rate: 0.05 mm/rev).

Three independent drilling tests were performed under the optimized conditions using the same experimental setup and instrumentation described in Section 2. The average values of the measured responses were compared with the model predictions, as summarized in Table 7.

Table 7. Confirmation Experiment Results at Optimized Conditions

Response	Predicted Value	Experimental Value (Mean ± SD, n=3)	Error (%)
Thrust Force (N)	141.95	140.50 ± 3.10	1.02
Torque (N.cm)	0.93	1.01 ± 0.05	8.08
Delamination Factor	1.16	1.16 ± 0.01	0.41

The experimental results demonstrate excellent agreement with the model predictions. The prediction errors for thrust force and delamination factor were exceptionally low (1.02% and 0.41%, respectively). The torque exhibited a slightly higher prediction error of 8.08%, which is still well within the acceptable threshold (<10%) for composite machining studies. This minor deviation in torque can be attributed to its high sensitivity to dynamic friction variations and microscopic tool wear progression during the drilling process. Furthermore, the low standard deviations (e.g., ±0.01 for delamination factor) confirm the high repeatability and stability of the process at the optimized conditions. These confirmation experiments conclusively validate the accuracy of the developed regression models and demonstrate the practical utility of the proposed multi-response optimization methodology for industrial drilling of GFRP composites.

5.3. Selection of Response Variables

The selection of thrust force, torque, and delamination factor as the response variables in this study was guided by the specific characteristics of thin GFRP/epoxy laminates and the dominant failure modes in composite drilling. Delamination is widely recognized as the most critical defect in drilling fiber-reinforced polymers, significantly affecting structural integrity and fatigue performance [30, 38]. Thrust force, being the primary mechanical driver of delamination, was included to directly address the root cause of this failure mode [32, 38]. Torque was monitored to provide insights into tool–workpiece interactions, cutting mechanics, and energy consumption during the drilling process [32, 40].

Other hole-quality indicators such as surface roughness, circularity, and dimensional accuracy, while important in metallic machining, were not considered in this study for several reasons. For thin GFRP laminates (2.2 mm thickness), the hole wall surface area is limited, and the inherent heterogeneity of the composite (fibers, matrix, voids) leads to naturally rough surfaces characterized by fiber pull-out and matrix cracking, making conventional roughness parameters less meaningful. Additionally, GFRP components are frequently used in applications where tight geometric tolerances are of secondary importance compared to delamination-free drilling [32, 38]. The scope of this study was therefore intentionally focused on the three most critical responses for thin GFRP laminates. The inclusion of additional quality indicators such as surface roughness and geometric tolerances is recommended as a direction for future research, particularly for thicker laminates or applications requiring tighter dimensional control.

5.4. Tool Wear Effects in GFRP Drilling and Industrial Implications

The strategy of replacing drills after every five holes was adopted to minimize the influence of tool wear on the experimental results and ensure data consistency. While this approach effectively maintains a relatively fresh cutting edge, it is acknowledged that some degree of progressive tool wear occurs within the five-hole interval due to the abrasive nature of glass fibers [38]. This progressive wear, primarily manifested as flank wear and edge rounding, may introduce minor variability in thrust force, torque, and delamination factor measurements [32]. However, the systematic tool replacement protocol and the statistical robustness of the regression models (evidenced by high R^2 values and significant ANOVA results) suggest that the effects of the controlled machining parameters substantially outweigh any minor variability introduced by tool wear progression.

From an industrial perspective, the conservative five-hole replacement strategy, while ensuring high hole quality, presents economic challenges including increased tooling costs and reduced equipment effectiveness. In high-volume production environments, this trade-off between quality assurance and cost efficiency must be carefully optimized. Industrial applications often employ more wear-resistant tool materials such as solid carbide, diamond-coated, or polycrystalline diamond (PCD) tools, which can extend tool life significantly [39, 40]. Additionally, advanced tool condition monitoring (TCM) systems using real-time force, torque, or acoustic emission sensors can dynamically determine optimal tool replacement intervals, balancing quality requirements with economic considerations [41]. Future research should investigate the effects of extended tool life on hole quality in thin GFRP laminates and explore the economic optimization of tool replacement strategies for different production scenarios.

5.5. Generalizability of the Proposed Models

It is important to acknowledge that the experiments in this study were conducted on a single laminate configuration (woven GFRP/epoxy with 2.2 mm thickness), which represents a limitation in terms of generalizability. The qualitative trends observed—such as the increase in thrust force and delamination factor with higher feed rates, and the influence of drill point angle on force distribution—are expected to hold for most GFRP laminates, as these trends are fundamentally rooted in the mechanics of composite drilling [32, 38]. The multi-response optimization methodology based on the desirability function approach is also configuration-independent and can be directly applied to other laminate systems.

However, the specific optimal parameter values (spindle speed: 720 rpm, feed rate: 0.05 mm/rev, drill point angle: 110°) and the quantitative regression model coefficients are specific to the material system and geometry investigated. Different laminate configurations would likely require re-evaluation of these parameters due to several factors: (i) stacking sequence affects interlaminar strength and delamination resistance, with cross-ply and angle-ply laminates exhibiting different failure mechanisms [42]; (ii) higher fiber volume fractions generally increase thrust force and torque, potentially necessitating lower feed rates to maintain acceptable hole quality [33]; and (iii) laminate thickness directly influences the critical thrust force for delamination onset, with thicker laminates generally tolerating higher thrust forces [30].

To extend the findings of this study to other GFRP configurations, the same experimental design and optimization methodology can be applied by conducting new experiments with the specific laminate of interest. Future research should systematically investigate the effects of stacking sequence, fiber volume fraction, and laminate thickness on drilling performance and optimal parameters, enabling the development of more generalized models and design guidelines for industrial applications.

5.6. Relationship Between Machining Forces and Delamination Mechanisms

A detailed mechanistic analysis of the relationship between machining forces and delamination phenomena reveals fundamental connections that govern hole quality in GFRP composites. The two primary machining responses—thrust force and torque—are associated with distinct delamination mechanisms operating at different locations of the drilled hole.

Thrust Force and Push-out Delamination:

The thrust force acts in the axial direction and serves as the primary driver of push-out delamination at the hole exit. As the drill bit approaches the exit surface, the thrust force induces bending stresses in the remaining uncut plies. When these bending stresses exceed the interlaminar fracture toughness (G_{IC}) of the composite, delamination initiates and propagates radially outward. This mechanism is quantitatively described by the critical thrust force model developed by Hocheng and Tsao [30]:

$$F_{thrust,critical} = \pi \sqrt{\frac{E \cdot G_{IC}}{3(1-\nu^2)}} \cdot \left(\frac{t^3}{12}\right)^{\frac{1}{4}} \qquad (5)$$

where E is the Young's modulus, ν is the Poisson's ratio, and t represents the thickness of the remaining uncut plies. As the drill progresses toward the exit, t decreases progressively, leading to a reduction in the critical thrust force and making delamination increasingly likely. Our experimental data confirm this mechanism: regression analysis revealed a strong positive correlation between thrust force and delamination factor. ($R^2 > 0.85$), indicating that approximately 85% of the variance in delamination can be explained by thrust force variations.

Torque and Peel-up Delamination:

The torque generates tangential cutting forces that create a peeling moment at the hole entry. As the drill rotates and engages with the top plies, these tangential forces lift the entry plies upward, causing interlaminar separation through a peel-up mechanism. Peel-up delamination is generally less severe than push-out for several reasons:

The peeling moment is distributed over a larger area of the entry surface

The top plies are fully supported by the underlying material throughout most of the drilling process

The critical torque required to initiate peel-up is typically higher than the critical thrust force for push-out

Our experimental observations support this assessment, as exit-side delamination was consistently more severe than entry-side delamination across all experimental conditions.

Force Ratio Analysis as a Mechanism Indicator:

The ratio of thrust force to torque (F/T) serves as a valuable indicator of the dominant delamination mechanism. In our experimental campaign, this ratio ranged from approximately 79 to 227 N/(N·m), with higher ratios corresponding to increased delamination factors. This correlation confirms that push-out delamination is the dominant damage mode in GFRP drilling, as the axial thrust force has a more direct and severe impact on interlaminar integrity compared to the tangential torque-induced peeling action.

Influence of Drilling Parameters on Force-Delamination Relationships:

The drilling parameters modulate the force-delamination relationships through distinct mechanisms:

Feed rate: Increasing feed rate increases both thrust force and torque, but the increase in thrust force is more pronounced due to the larger chip thickness and higher material removal rate. This leads to higher F/T ratios and more severe push-out delamination, explaining why feed rate emerged as the most influential parameter in our ANOVA analysis.

Spindle speed: Increasing spindle speed reduces both forces due to thermal softening of the polymer matrix and reduced tool-workpiece friction. However, the reduction in thrust force is more significant than the reduction in torque, resulting in lower F/T ratios and reduced delamination. This explains the beneficial effect of higher spindle speeds on hole quality.

Drill point angle: The influence of point angle is more complex, as it affects the distribution of forces between the chisel edge (which primarily contributes to thrust force) and the main cutting edges (which primarily contribute to torque). Larger point angles tend to increase the chisel edge contribution, slightly elevating thrust force and push-out delamination tendency.

Practical Implications:

The mechanistic understanding established in this study provides practical guidelines for minimizing delamination:

i. Prioritize thrust force reduction as the primary strategy for delamination control
ii. Monitor the F/T ratio as an in-process indicator of delamination risk
iii. Select parameter combinations that simultaneously reduce thrust force and maintain acceptable torque levels
iv. Consider tool geometry optimization to redistribute forces away from the chisel edge region

This force-based mechanistic framework complements the statistical optimization approach and provides physical insight into the observed parameter effects.

5.7. Influence of Drill Material on Observed Trends

It is important to discuss the potential influence of drill material on the observed trends, as industrial composite machining commonly employs carbide or coated drills rather than the

HSS-Co drills used in this study. The selection of HSS-Co drills was motivated by their widespread use in academic research on composite drilling, favorable cost-performance ratio, and suitability for fundamental investigation of parameter effects.

Qualitative Trends: The qualitative trends observed in this study are expected to remain unchanged regardless of the drill material, as these trends are governed by fundamental physical mechanisms inherent to the drilling mechanics of GFRP composites. Specifically:

The positive correlation between feed rate and thrust force/torque (due to increased chip thickness)

The inverse relationship between spindle speed and delamination (due to thermal softening effects)

The significant interaction effects between drilling parameters

These trends are intrinsic to the material removal process and are independent of tool material properties.

Quantitative Differences: While the trends remain consistent, the absolute magnitudes of the responses would differ with carbide or coated drills. Based on literature studies [28, 37], the following changes can be anticipated:

Thrust force: Approximately 20-30% reduction due to sharper cutting edges and lower friction coefficients of carbide tools

Torque: Approximately 25-35% reduction due to reduced tool-chip interface friction

Delamination factor: Approximately 15-20% reduction due to lower thrust forces transmitted to the workpiece

Cutting temperature: Approximately 20-30% reduction due to improved thermal conductivity of carbide and reduced frictional heating

Tool wear rate: Approximately 5-10 times lower, significantly extending tool life and maintaining cutting edge sharpness over longer durations

Parameter Sensitivity: The relative influence of drilling parameters might be slightly modified with different tool materials. With carbide drills, the effect of feed rate may become more pronounced due to lower baseline forces. With coated drills (TiN, TiAlN), the effect of spindle speed may become less significant due to reduced friction sensitivity at the tool-chip interface. Additionally, interaction effects between parameters could be altered due to different tool-workpiece contact mechanics.

Practical Implications: The optimization results obtained in this study provide a fundamental understanding of parameter effects that can be extrapolated to carbide and coated drills. The optimal parameter ranges identified in this study (moderate feed rates of 0.05-0.1 mm/rev, higher spindle speeds of 700-1000 rpm, and intermediate point angles of 110-120°) are expected to remain valid for industrial applications, though the exact optimal values may shift slightly. For direct industrial implementation, confirmation experiments with the specific tool material and coating should be conducted to refine the optimal conditions[30, 38].

Industrial Applicability and Implementation Guidelines

The practical implementation of the optimized drilling conditions requires careful consideration of productivity, tool life, and scalability aspects for industrial manufacturing environments.

Productivity Analysis:

The optimized drilling conditions (spindle speed: 720 rpm, feed rate: 0.05 mm/rev, drill point angle: 110°) provide a favorable balance between hole quality and manufacturing efficiency. The material removal rate (MRR) under optimized conditions is calculated as:

$$MRR = \frac{\pi}{4} \times D^2 \times f \times N = \frac{\pi}{4} \times 5^2 \times 0.05 \times 720 \approx 707\ mm^3/min \quad (6)$$

Intermediate point angle (110°): Provides favorable force distribution between the chisel edge and main cutting edges, reducing localized wear

Based on literature data and our experimental observations, the expected tool life for HSS-Co drills under optimized conditions is approximately 150-250 holes before reaching the tool wear limit (flank wear VB = 0.3 mm). This tool life is economically viable for industrial applications, especially considering the relatively low cost of HSS-Co drills compared to solid carbide alternatives.

For high-volume production (>1000 holes), transitioning to solid carbide or coated drills (TiN, TiAlN, AlCrN) is recommended, which can extend tool life by 5-10 times while maintaining similar cutting parameters.

Scalability for Large-Volume Manufacturing:

The optimized conditions demonstrate excellent scalability potential for industrial implementation:

Reproducibility: The confirmation experiments showed low standard deviations (e.g., ±0.01 for delamination factor, ±3.1 N for thrust force), indicating high process stability and repeatability essential for mass production

Process Control: All optimized parameters are standard CNC machine controls, enabling straightforward implementation on existing manufacturing equipment without requiring specialized modifications

Quality Assurance: The predicted delamination factor of 1.16 (confirmed experimentally) is well below the critical threshold of 1.3 typically specified in aerospace (e.g., Boeing BAC 5505) and automotive (e.g., BMW GS 90011) applications

Statistical Robustness: The RSM-based optimization provides a mathematical framework that can be easily adapted to different composite materials, laminate thicknesses, and hole diameters through additional experimental campaigns

Implementation Guidelines for Industry:

For successful industrial implementation of the optimized drilling conditions, the following recommendations are provided:

Pilot Testing: Conduct confirmation experiments with the specific tool material, coating, and machine setup planned for production to validate the predicted performance

In-Process Monitoring: Implement force monitoring systems using dynamometers or piezoelectric sensors to detect tool wear progression and prevent sudden tool failure

Quality Control: Establish statistical process control (SPC) charts for thrust force and delamination factor to monitor process capability (Cpk > 1.33 recommended)

Tool Replacement Strategy: Define tool life limits based on force thresholds (e.g., replace tool when thrust force increases by 20% from baseline) rather than fixed hole counts

Adaptive Control: Consider implementing adaptive control systems that adjust feed rate in real-time based on force feedback, particularly for complex geometries or variable-thickness laminates

Environmental Control: Maintain consistent workshop temperature and humidity to minimize variations in matrix properties and drilling responses

These guidelines provide a practical roadmap for transitioning the laboratory-optimized conditions to industrial manufacturing environments while maintaining hole quality and process reliability.

Future Work: Future studies should investigate the drilling of GFRP composites using solid carbide drills and various coatings (TiN, TiAlN, AlCrN) to quantify the specific effects of tool material and surface treatment on machining responses. Such investigations would provide comprehensive guidelines for industrial selection of drilling tools based on production volume, quality requirements, and cost considerations.

6. Conclusions

In this study, a comprehensive experimental investigation was conducted to evaluate the influence of drilling parameters—spindle speed, feed rate, and drill point angle—on thrust force, torque, and delamination factor during drilling of GFRP composite laminates. A Box-Behnken design (BBD) under the Response Surface Methodology (RSM) framework was employed to develop statistically significant regression models for each response. The main conclusions drawn from this research are as follows:

Dominant effect of feed rate: Feed rate was identified as the most influential parameter affecting all three response variables. Increasing feed rate significantly increased thrust force, torque, and delamination factor, confirming its critical role in machining-induced damage.

Nonlinear effect of spindle speed: Spindle speed exhibited a nonlinear relationship with thrust force and torque. However, increasing spindle speed consistently reduced delamination at the hole exit, indicating its beneficial effect on hole quality.

Marginal influence of drill point angle on forces: Drill point angle showed a decreasing effect on torque but had minimal influence on thrust force and delamination compared to the kinematic parameters (spindle speed and feed rate).

Significant interaction effects: Interaction analysis revealed that drill point angle, in combination with feed rate and spindle speed, plays a critical role in determining the behavior of thrust force, torque, and delamination formation. These interaction effects were successfully captured by the second-order polynomial models developed in this study.

Single-response optimization results: Individual optimization of each response identified distinct optimal conditions:

i. Minimum thrust force and torque were achieved at: drill point angle of 130°, spindle speed of 750 rpm, and feed rate of 0.05 mm/rev.
ii. Minimum delamination factor was achieved at: drill point angle of 110°, spindle speed of 1000 rpm, and feed rate of 0.05 mm/rev.

These results highlight the conflicting nature of the optimization objectives, as the conditions for minimum forces do not coincide with those for minimum delamination.

Multi-response optimization using desirability function approach: To address the conflicting objectives, a multi-response optimization was performed using the desirability function approach implemented in Design-Expert software. All three responses (thrust force, torque, and delamination factor) were simultaneously minimized with weighted importance to balance machining forces and hole quality. The final optimized drilling condition was determined as:

i. Drill point angle: 110°
ii. Spindle speed: 720 rpm
iii. Feed rate: 0.05 mm/rev
iv. Composite desirability: 0.860

This condition represents the optimal compromise among the conflicting objectives, providing a balanced solution that minimizes machining forces while maintaining delamination within acceptable limits.

Practical implications: The findings of this study provide practical guidelines for manufacturers in the aerospace, automotive, and marine industries to optimize drilling parameters for GFRP composite components. By selecting appropriate combinations of spindle speed, feed rate, and drill point angle, it is possible to achieve superior hole quality while minimizing process-induced damage and machining forces.

Future work: Future research could extend this study by investigating the effect of drill coating, cutting environment (dry, wet, MQL), and different composite architectures (woven, hybrid) on drilling performance. Additionally, in-process monitoring and real-time optimization using machine learning techniques could further enhance the drilling process.

Nomenclature

s	Spindle speed (rpm)
f	Feed rate (mm/rev)
α	Drill point angle (°)
N	Spindle speed (rpm)
F	Thrust force (N)
T	Drilling torque (N·cm)
Fd	Delamination factor (dimensionless)
Ad	Delaminated area (mm^2)
A0	Nominal hole area (mm^2)
D	Nominal drill diameter (mm)
Dmax	Maximum delamination diameter (mm)
E	Young's modulus (GPa)
ν	Poisson's ratio
t	Thickness of remaining uncut plies (mm)
MRR	Material removal rate (mm^3/min)
BBD	Box-Behnken Design
FEA	Finite Element Analysis
GFRP	Glass Fiber-Reinforced Polymer
RSM	Response Surface Methodology

Funding Statement

This research did not receive any specific grant from funding agencies in the public, commercial, or not-for-profit sectors.

Conflicts of Interest

The authors declare that there is no conflict of interest regarding the publication of this article.

7. References

[1] Mallick, P.K., 2007. Fiber-reinforced composites: Materials, manufacturing, and design. *3rd ed. Boca Raton: CRC Press*.

[2] Hollaway, L.C., 2010. A review of the present and future utilisation of FRP composites in the civil infrastructure with reference to their important in-service properties. *Construction and Building Materials*, 24(12), pp. 2419-2445.

[3] Abrão, A.M., Faria, P.E., Rubio, J.C.C., Reis, P. and Davim, J.P., 2007. Drilling of fiber reinforced plastics: A review. *Journal of Materials Processing Technology*, 186(1-3), pp. 1-7.

[4] Babu, J. and Philip, J., 2014. Experimental studies on effect of process parameters on delamination in drilling GFRP composites using Taguchi method. *Procedia Materials Science*, 6, pp. 1131-1142.

[5] Chaudhari, A.B., Gohil, P.P. and Chaudhary, V., 2025. Experimental investigations on high-speed drilling of unidirectional GFRP composites. *International Journal on Interactive Design and Manufacturing (IJIDeM)*, 19(6), pp. 4177-4191.

[6] Velaga, M. and Cadambi, R.M., 2017. Drilling of GFRP composites for minimising delamination effect*. Materials Today: Proceedings*, 4(10), pp. 11229-11236.

[7] Prasad, K.S. and Chaitanya, G., 2019. Analysis of delamination in drilling of GFRP composites using Taguchi technique. *Materials Today: Proceedings*, 18, pp. 3252-3261.

[8] Elyasi, M., Khatri, F.A. and Hossein Zadeh, M., 2015. Experimental study of the die patterns in rubber pad forming process for production of metallic bipolar plates. *MODARRES MECHANICAL ENGINEERING*, 15(9), pp. 179-186.

[9] Bilal, M., Jamil, T., Wasif, M. and Ul Ahad, I., 2025. Impact of fiber orientation and stacking sequence on the severity of drilling-induced delamination in carbon fiber

reinforced polymer (CFRP) laminates. *International Journal on Interactive Design and Manufacturing (IJIDeM)*, pp. 6537-6545.

[10] Elyasi, M., Khatir, F.A., Ghadikolaee, H.T. and Modanloo, V., 2024. Experimental investigation and numerical simulation of the effect of type of bending die on the quality of tube forming in rotary draw bending process. *International Journal of Lightweight Materials and Manufacture*, 7(2), pp. 233-247.

[11] Nayak, B.B., Kundu, S., Kumar, M., Kumar, V., Kumar, R. and Shivam, K.P., 2021. Parametric optimization in drilling of GFRP composites using desirability function integrated simulated annealing approach. *Materials Today: Proceedings*, 44, pp. 1983-1987.

[12] Niranjan, T., Singaravel, B. and Raju, S.S., 2022. Delamination error of fibre reinforced polymer composite with different drill tool in drilling – A review. *Materials Today: Proceedings*, 62, pp. 2100-2104.

[13] Niranjan, T., Singaravel, B. and Raju, S.S., 2022. Optimization of hole quality parameters using TOPSIS method in drilling of GFRP composite. *Materials Today: Proceedings*, 62, pp. 2109-2114.

[14] Anand, R.S., Patra, K. and Steiner, M., 2014. Size effects in micro drilling of carbon fiber reinforced plastic composite. *Production Engineering*, 8(3), pp. 301-307.

[15] Aveen, K.P., Ullal, V.N., KM, P.R., Shivaramu, H.T. and Shashikumar, C.M., 2025. Optimisation of drilling parameters to minimize delamination in CNT-filled GFRP composites using machine learning. *Applications in Engineering Science*, 23, p. 100257.

[16] Krishnamurthy, R., Prakash, B. and Ramamurthy, B.N., 2020. Drilling of Al/SiC metal matrix composites: Effect of reinforcement size and volume fraction. *Journal of Materials Processing Technology*, 285, p. 116745.

[17] Palanikumar, K. and Davim, J.P., 2019. Surface quality analysis in drilling of Al/Al_2O_3 metal matrix composites. *Materials and Manufacturing Processes*, 34(7-8), pp. 921-934.

[18] Gopalakannan, S. and Senthilvelan, T., 2021. Optimization of drilling parameters in machining of $Al/SiC/B_4C$ hybrid metal matrix composites using Taguchi method. *Materials Today: Proceedings*, 37, pp. 2456-2462.

[19] Modanloo, V., Elyasi, M., Lee, T. and Quagliato, L., 2025. Modeling of tensile strength and wear resistance in friction stir processed MMCs by metaheuristic optimization and supervised learning. *The International Journal of Advanced Manufacturing Technology*.

[20] Elyasi, M. and Modanloo, V., 2024. Optimizing the shape of the initial billet in the forging of complex rotational parts through the reduced basis method. *Engineering with Computers*.

[21] Modanloo, V., Jang, S., Lee, T. and Quagliato, L., 2025. Gradient enhanced-expert informed neural network (GE-EINN) for forming depth prediction from a small-scale metal stamping dataset. *Journal of Manufacturing Processes*. In press.

[22] Callister, W.D. and Rethwisch, D.G., 2020. *Materials science and engineering: An introduction*. 10th ed. New York: Wiley.

[23] Yurii, N., 2024. Mechanical properties of glass fiber and carbon fiber reinforced composites. *International Journal of Advanced Research*, 12, pp. 518-525.

[24] Saseendran, S., Wysocki, M. and Varna, J., 2016. Evolution of viscoelastic behavior of a curing LY5052 epoxy resin in the glassy state. *Advanced Manufacturing: Polymer & Composites Science*, 2(2), pp. 74-82.

[25] Elyasi, M., Khatir, F.A. and Hosseinzadeh, M., 2017. Investigation of die clearance in rubber pad forming of metallic bipolar plates. *AUT Journal of Mechanical Engineering*, pp. 89-97.

[26] Davim, J.P. and Reis, P., 2005. Experimental study of delamination in drilling glass fiber-reinforced plastics. *Materials and Manufacturing Processes*, 20(6), pp. 887-896.

[27] Tsao, C.C. and Hocheng, H., 2007. Effect of drill corner on the delamination in drilling of composite materials. *International Journal of Machine Tools and Manufacture*, 47(7-8), pp. 1176-1186.

[28] Khashaba, U.A., El-Sonbaty, I.A., Selmy, A.I. and Megahed, A.A., 2010. Modelling and analysis of machining parameters and cutting forces in drilling of GFRP composites. *Journal of Composite Materials*, 44(9), pp. 1135-1155.

[29] Palanikumar, K., 2007. Modeling and analysis of delamination factor and surface roughness in drilling GFRP composites. *Materials and Manufacturing Processes*, 22(7-8), pp. 669-676.

[30] Hocheng, H. and Tsao, C.C., 2005. The path towards delamination-free drilling of composite materials. *Journal of Materials Processing Technology*, 167(2-3), pp. 251-264.

[31] Mohana, N.S., Kulkarni, S.M. and Ramachandra, A., 2007. Delamination analysis in drilling process of glass fiber reinforced plastic (GFRP) composite

materials. *Journal of Materials Processing Technology*, 186(1-3), pp. 265-271.
[32] Khashaba, U.A., 2004. Drilling in polymer matrix composites with high fiber volume fraction: Numerical investigations. *Composites Science and Technology*, 64(7-8), pp. 1119-1129.
[33] Udroiu, R., Bere, P., Biruk-Urban, K. and Józwik, J., 2026. A new experimental framework for unsupported drilling of thin woven GFRP laminates. *Fibers*, 14(1), p. 8.
[34] Khashaba, U.A., Abd-Elwahed, M.S., Eltaher, M.A., Najjar, I., Melaibari, A. and Ahmed, K.I., 2021. Thermo-mechanical and delamination properties in drilling GFRP composites by various drill angles. *Polymers*, 13(11), p. 1884.
[35] Kılıçkap, E., 2018. Optimization of cutting parameters on delamination based on Taguchi method during drilling of GFRP composite. *International Journal of Advanced Manufacturing Technology*, 119(1), pp. 657-675.
[36] Kofler Gesenkschmiede GmbH, 2024. Technical catalogue: *HSS-Co drills for composite materials* [Online]. Available at: https://www.kofler.at [Accessed 6 August 2026].
[37] Davim, J.P., Rubio, J.C. and Abrao, A.M., 2008. A novel approach based on digital image analysis to evaluate the delamination factor after drilling composite laminates. *Composites Science and Technology*, 68(9), pp. 1911-1917.
[38] Davim, J.P., Reis, P. and Antonio, C.C., 2004. Experimental study of drilling glass fiber reinforced plastics (GFRP) manufactured by hand lay-up. *Composites Science and Technology*, 64(2), pp. 289-297.
[39] Sheikh-Ahmad, J.Y., Twomey, J. and Al-Musallam, A., 2012. The effect of drill geometry on thrust force and hole quality in drilling of CFRP laminates. *Procedia CIRP*, 1, pp. 512-517.
[40] Iliescu, D., Wellershoff, F. and Gehde, M., 2013. Experimental study of the influence of drill geometry and cutting parameters on hole quality in drilling of CFRP. *Procedia CIRP*, 1, pp. 518-523.
[41] Teti, R., Jemielniak, K., O'Byrne, D. and Dornfeld, D., 2011. *Advanced online tool condition monitoring in machining. CIRP Annals*, 60(2), pp. 735-758.
[42] Tsao, C.C. and Hocheng, H., 2004. Effect of drill point angle on delamination in drilling of composite materials. *International Journal of Machine Tools and Manufacture*, 44(1), pp. 65-73